Electronic Supplementary Material (ESI) for RSC Advances.
This journal is © The Royal Society of Chemistry 2019

Heterogeneous Biochars from Agriculture Residues and Coal Fly Ash for the Removal of Heavy Metals from Coking Wastewater

Lihui Gao[1,2,3*] and Jillian L. Goldfarb[2,3,4]

1. School of Chemical Engineering and Technology, China University of Mining and Technology, Xuzhou 221116, People's Republic of China
2. Department of Mechanical Engineering, Division of Materials Science and Engineering, Boston University, 110 Cummington Mall, Boston MA 02215 USA
3. The Leone Family Department of Energy & Mineral Engineering, The EMS Energy Institute, and The Institutes of Energy and the Environment, The Pennsylvania State University, University Park, PA 16802, United States
4. Department of Biological and Environmental Engineering, Cornell University, 226 Riley-Robb Hall, Ithaca NY 14853

Supplemental Information (for online publication only)

Figure S1	Image of coking wastewater prior to biological treatment	S1
Table S1	Composition of wheat straw samples from across the globe as reported in the literature	S2
Table S2	Representative proximate and ultimate analysis of global bituminous coals	S3
Table S3	Representative heavy metal contents in global samples of coal fly ashes from bituminous coals	S4
Table S4	Results ICP-MS analysis of heavy metals present in coking wastewater before and after biological treatment	S5
Figure S2	XPS wide energy spectrums of biochar and activated carbon	S6
Figure S3	C1s peaks of biochar and activated carbon	S7
Figure S4	Adsorption kinetic data of heavy metals to biochars and activated carbons	S8
Table S5	Adsorption kinetic data fit to pseudo-first order, pseudo-second order and intraparticle diffusion models (± 1 standard error)	S9
Table S6	Adsorption isotherm data fit to Langmuir, Freundich and Temkin models (± 1 standard error)	S10
References		S11

[*] To whom correspondence should be addressed: lihuigaocumt@163.com

Figure S1. Image of coking wastewater prior to biological treatment

Table S1. Composition of wheat straw samples from across the globe as reported in the literature

	USA (This Study)	Australia[1]	Mexico[2]	Canada[3]	China[4]	China[4]	India[5]
Proximate Analysis				**Average Wt % (dry basis)**			
Volatile Matter	86.09 ± 0.79	76.3	68.23	77.04-79.85	63.96 ± 7.29	68.45	83.08
Fixed Carbon	9.27 ± 0.89	18.5	14.72	16.76-18.15	14.96 ± 1.49	15.12	10.29
Ash (Inorganic Matter)	4.64 ± 0.11	5.2	17.04	3.09-4.81	12.45 ± 9.02	6.29	6.63
Ultimate Analysis				**Average Wt % (dry basis)**			
C	53.94 ± 0.56	46	37.2	44.26 - 46.04	42.11 ± 2.12	50.02	38.34
H	5.93 ± 0.01	5.92	5.57	4.97 - 5.92	6.53 ± 0.46	5.33	5.47
N	0.70 ± 0.09	1.42	1.14	0.34 - 1.16	0.58 ± 0.28	0.67	0.60
O	39.32 ± 0.63	41.3	37.3	43.79 - 44.48	40.51 ± 2.67	43.75	55.22
S	0.11 ± 0.01	0.15	0.2	0.08 - 0.13	0.32 ± 0.10	0.23	0.37

Table S2. Representative proximate and ultimate analysis of global bituminous coals

	Venezuela (This Study)	Pennsylvania USA[6]	Henan Province, China[7]			Shaanxi, China[7]
Proximate Analysis	**Average Wt % (dry basis)**					
Volatile Matter	36.3	32.18	41.49	37.91	35.98	30.56
Fixed Carbon	63.63	60.88	39.23	43.63	44.22	49.88
Ash (Inorganic Matter)	0.07	6.93	18.51	17.30	18.75	15.38
Ultimate Analysis	**Average Wt % (dry basis)**					
C	76.9	76.28	68.95	68.88	67.03	79.31
H	5.36	5.33	5.14	5.45	5.34	4.72
N	1.35	1.42	1.11	0.13	1.09	1.03
O	8.74	7.65	5.52	7.08	6.74	13.38
S	0.64	1.73				1.30
HHV (MJ/kg)	28.85	30.93				25.44

Table S3. Representative heavy metal contents in global samples of coal fly ashes from bituminous coals

Wt % in Fly Ash	**Venezuela (This Study)**			**Huaibei, China[8]***		**Poland[9]***	**Canada[10]***	
Al	12.93	±	3.18	15.25	17.78	8.16	12.01	10.21
Ba	1.65	±	0.08				0.21	0.15
Br	0.42	±	0.07					
Ca	1.38	±	3.01	3.96	3.81	6.19	1.84	2.07
Cr							0.03	0.02
Fe	1.49	±	2.64	4.82	6.22	4.34	2.52	2.98
K	1.54	±	3.65	0.64	1.00	1.37	1.92	1.62
Mg	0.46	±	0.77	1.20	0.80	2.84	0.67	0.69
Mn	0.05	±	0.01			0.02	0.03	
Na	4.94	±	7.69	0.52	0.33	1.61	0.37	0.30
Ni							0.01	0.01
P	0.49	±	0.03	0.23	0.18	0.38	0.20	0.10
S	2.36	±	3.39	1.36	1.49	1.69	0.25	0.24
Si	8.48	±	0.08	24.75	22.14	10.92	26.18	27.03
Sr							0.29	0.03
Ti	12.39	±	10.05	0.80	0.81	0.46	0.55	0.44
V							0.02	0.02

Wt % in Fly Ash	**U.S.-Fired Coals[11]**				
Al	12.34	14.32	13.87	15.44	9.80
Ba	0.05	0.08	0.12	0.08	0.05
Br					
Ca	1.94	0.88	1.21	0.44	1.80
Cr					
Fe	10.28	9.68	10.16	2.25	24.37
K	1.34	1.91	2.00	2.19	0.98
Mg	0.43	0.46	0.47	0.48	0.37
Mn					
Na	0.35	0.13	0.10	0.18	0.26
Ni					
P	0.21	0.11	0.10	0.05	0.06
S	0.40	0.27	0.23	0.02	0.32
Si	21.76	22.66	23.42	26.84	19.23
Sr					
Ti	0.79	0.95	0.99	1.17	0.55
V					

*Calculated from chemical composition of minerals

Table S4. Results ICP-MS analysis of heavy metals present in coking wastewater before and after biological treatment

	As (ppm)	Cd (ppm)	Co (ppm)	Cr (ppm)	Cu (ppm)
Coking wastewater	0.101±0.414	0.101±0.342	1.049±0.159	0.107±0.247	0.549±0.136
Water after Biological Treatment	0.035±1.287	0.028±0.310	0.107±0.075	0.010±0.251	0.861±0.454
	Mn (ppm)	**Ni (ppm)**	**Pb (ppm)**	**Se (ppm)***	**Zn (ppm)**
Coking wastewater	2.482±0.205	0.798±0.136	0.036±0.291	69.422±0.155	1.364±0.243
Water after Biological Treatment	0.748±0.120	0.077±0.180	0.084±0.350	13.031±0.332	1.368±0.231

** Note: high energy He mode not utilized; Se reported only for presence, but given Ar-Ar dimer interference, Se was not selected as model compound in adsorption experiments*

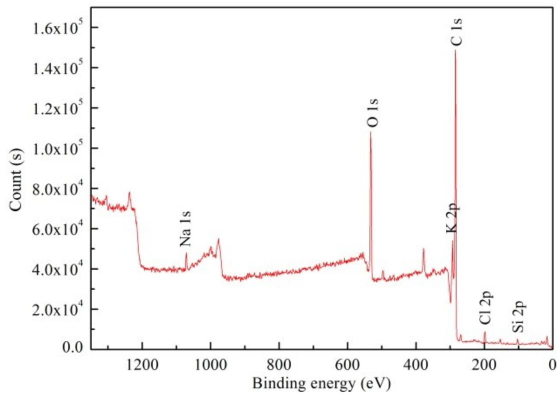

a. Py_WS

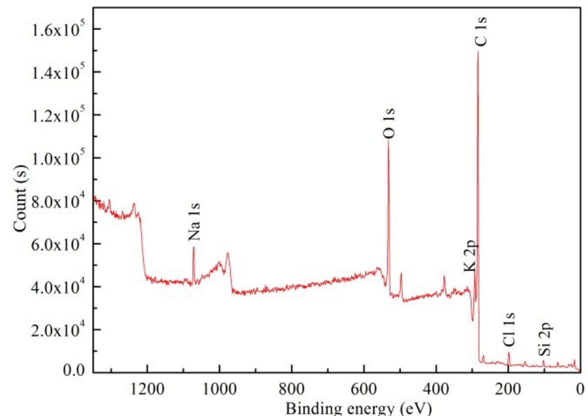

b. Py_WS_FA(20:1)

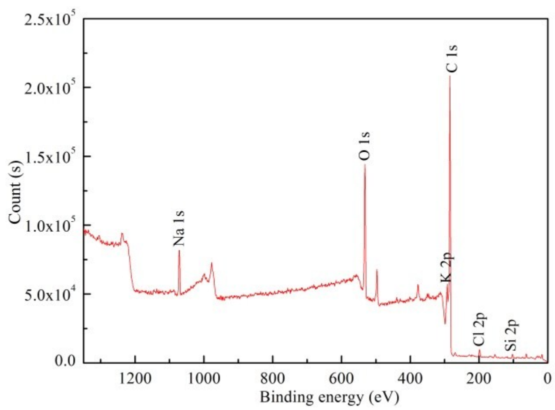

c. Py_WS_FA(10:1)

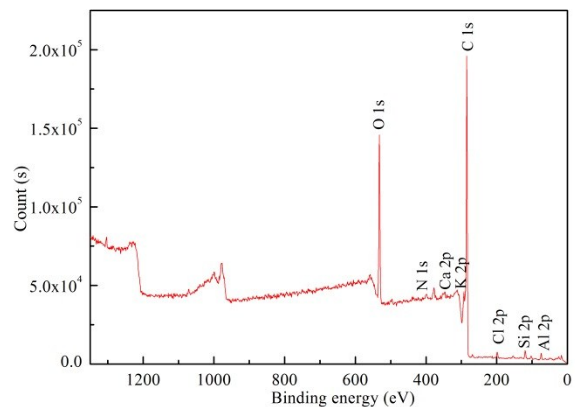

d. AC_ WS

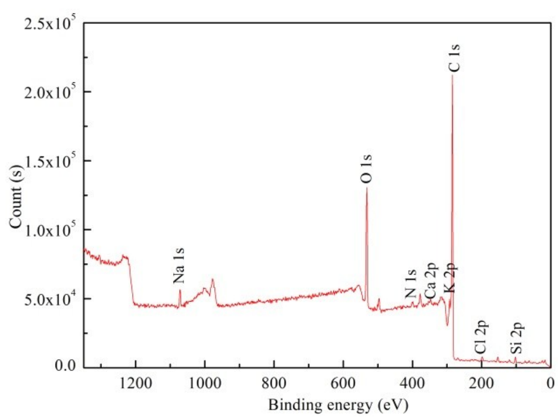

e. AC_WS_FA(20:1)

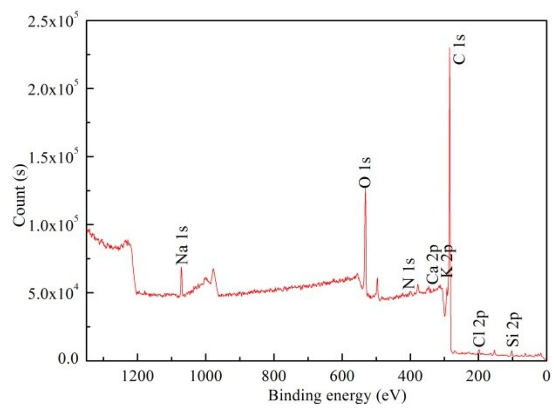

f. AC_WS_FA(10:1)

Figure S2. XPS wide energy spectrums of biochar and activated carbon

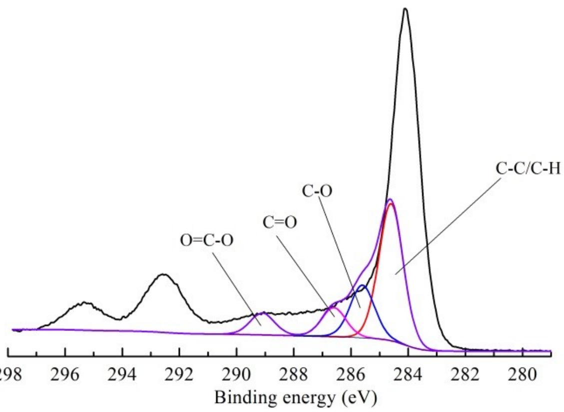

a. Py_WS

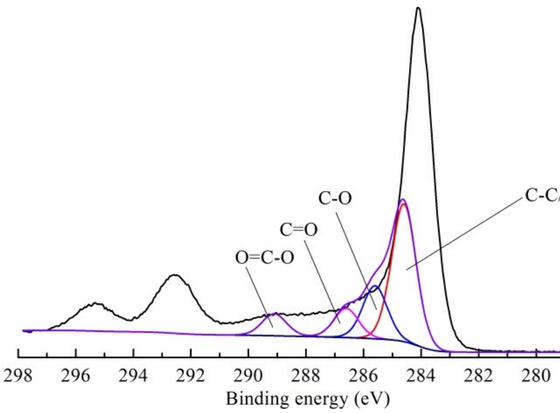

b. Py_WS_FA(20:1)

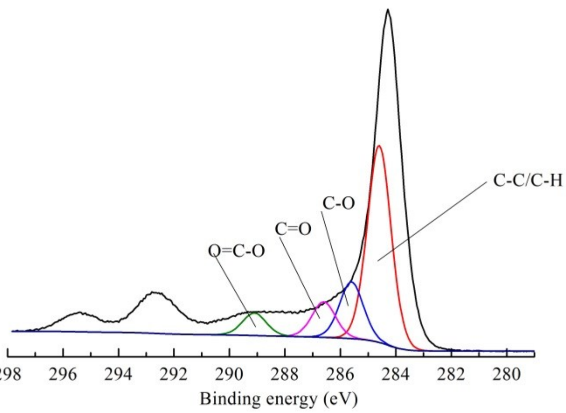

c. Py_WS_FA(10:1)

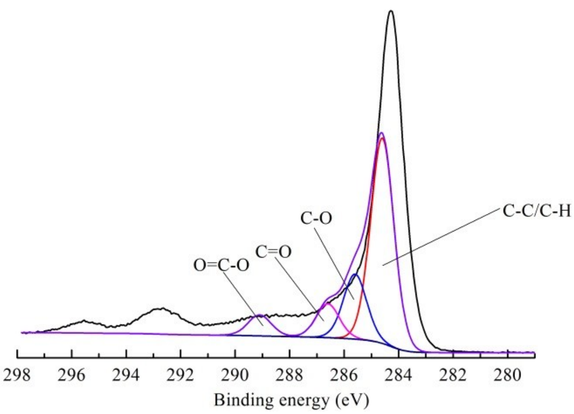

d. AC_ WS

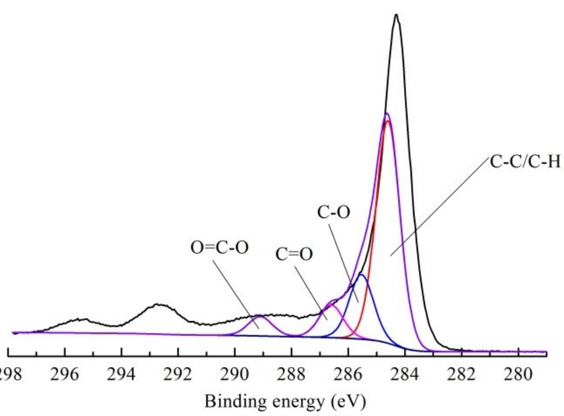

e. AC_WS_FA(20:1)

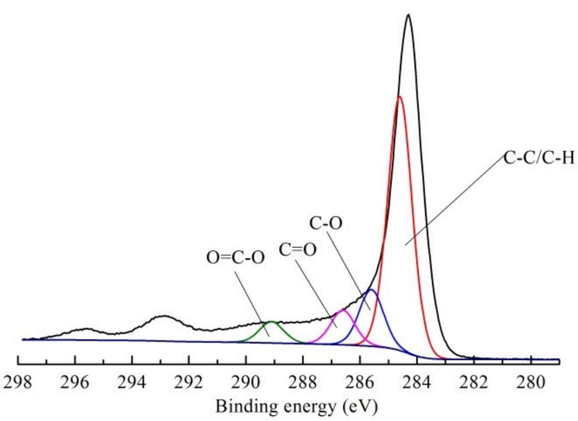

f. AC_WS_FA(10:1)

Figure S3. C1s peaks of biochar and activated carbon

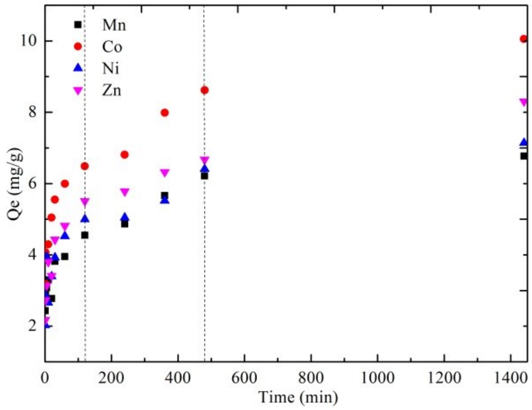

a. Py_WS

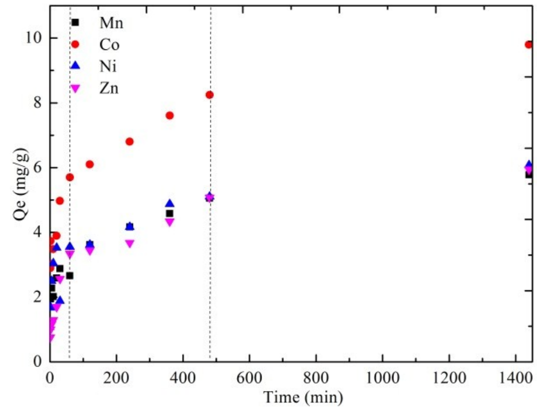

b. Py_WS_FA(20:1)

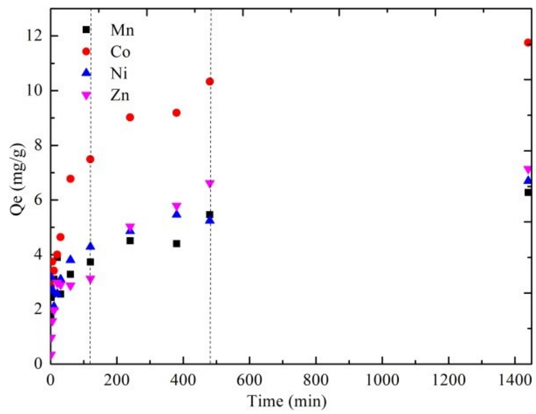

c. Py_WS_FA(10:1)

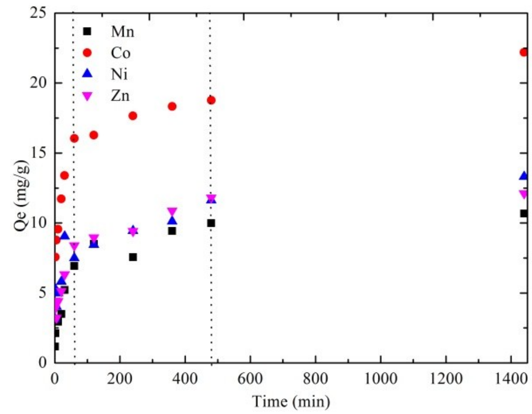

d. AC_ WS

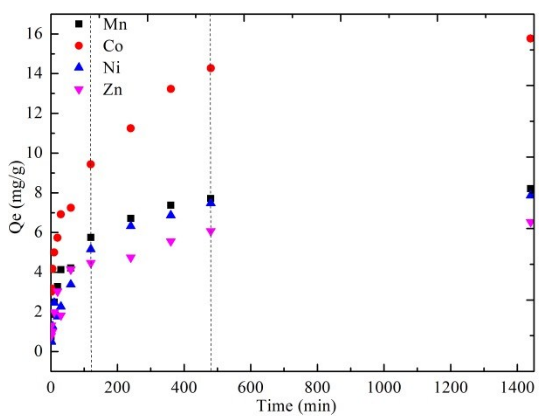

e. AC_WS_FA(20:1)

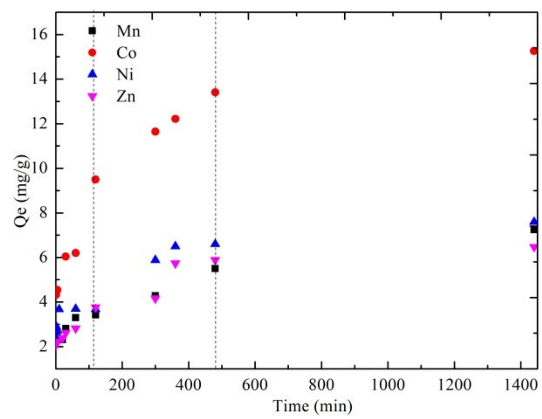

f. AC_WS_FA(10:1)

Figure S4. Adsorption kinetic data of heavy metals to biochars and activated carbons

Table S3. Adsorption kinetic data fit to pseudo-first order, pseudo-second order and intraparticle diffusion models (± 1 standard error)

Biochar	Metal	Pseudo-first-order kinetic			Pseudo-second-order kinetic			Intraparticle diffusion		
		K_1(1/min)	q_{e1}(mg/g)	R^2	K_2(g/mg min)	q_{e2}(mg/g)	R^2	K_i(mg/(g/min$^{0.5}$))	D(mg/g)	R^2
Py_WS	Mn	3.75E-03	3.845	0.965	4.45E-03	6.802	0.995	1.23E-01	2.852	0.903
	Co	2.85E-03	5.683	0.943	2.62E-03	10.030	0.991	1.82E-01	4.017	0.923
	Ni	3.16E-03	3.936	0.943	4.03E-03	7.138	0.991	1.28E-01	2.972	0.850
	Zn	2.49E-03	4.819	0.886	2.92E-03	8.246	0.989	1.57E-01	3.046	0.906
Py_WS_FA(20:1)	Mn	3.37E-03	3.700	0.967	4.12E-03	5.809	0.992	1.21E-01	1.917	0.901
	Co	2.90E-03	6.006	0.947	2.42E-03	9.787	0.991	1.95E-01	3.399	0.919
	Ni	2.87E-03	3.617	0.888	3.75E-03	6.088	0.990	1.17E-01	2.203	0.840
	Zn	3.23E-03	4.407	0.913	2.93E-03	5.988	0.986	1.46E-01	1.266	0.884
Py_WS_FA(10:1)	Mn	3.10E-03	3.639	0.915	4.35E-03	6.321	0.995	1.13E-01	2.445	0.850
	Co	3.55E-03	7.872	0.940	2.02E-03	11.817	0.994	2.67E-01	3.442	0.887
	Ni	2.54E-03	3.848	0.895	3.95E-03	6.754	0.994	1.22E-01	2.557	0.904
	Zn	4.48E-03	5.642	0.907	2.95E-03	7.254	0.996	1.86E-01	1.434	0.841
AC_WS	Mn	5.10E-03	7.140	0.914	3.34E-03	10.806	0.999	2.64E-01	3.000	0.771
	Co	3.15E-03	12.216	0.854	1.55E-03	22.090	0.995	4.31E-01	8.762	0.829
	Ni	3.21E-03	8.422	0.948	1.78E-03	13.342	0.991	2.72E-01	4.505	0.905
	Zn	6.03E-03	7.763	0.944	3.12E-03	12.238	0.998	2.63E-01	4.552	0.807
AC_WS_FA(20:1)	Mn	5.35E-03	5.827	0.976	3.64E-03	8.332	0.998	2.09E-01	2.258	0.809
	Co	4.21E-03	11.456	0.976	1.41E-03	15.982	0.998	3.80E-01	4.123	0.893
	Ni	5.77E-03	6.594	0.986	2.40E-03	8.111	0.997	2.28E-01	1.339	0.827
	Zn	4.74E-03	4.717	0.937	3.65E-03	6.627	0.995	1.66E-01	1.641	0.800
AC_WS_FA(10:1)	Mn	1.91E-03	4.684	0.943	2.02E-03	7.266	0.974	1.31E-01	2.258	0.949
	Co	3.56E-03	10.387	0.972	1.34E-03	15.423	0.992	3.35E-01	4.560	0.883
	Ni	3.55E-03	4.830	0.972	3.56E-03	7.628	0.995	1.55E-01	2.619	0.902
	Zn	3.63E-03	4.372	0.904	4.10E-03	6.565	0.995	1.37E-01	2.078	0.885

Table S4. Adsorption isotherm data fit to Langmuir, Freundich and Temkin models (± 1 standard error)

Biochar	Metals	Langmuir			Freundlich			Temkin		
		K_L（L/mg)	Q_m (mg/g)	R^2	K_f ($mg^{1-n}L^n/g$)	n	R^2	K_T(L/mol)	B(J/mol)	R^2
Py_WS	Mn	1.70E-02	6.316	0.997	1.128	3.949	0.952	4.13E-01	1.026	0.989
	Co	2.20E-03	37.405	0.998	0.456	1.724	0.983	2.65E-02	7.682	0.977
	Ni	9.10E-03	13.000	0.994	0.836	2.473	0.989	1.11E-01	2.571	0.978
	Zn	4.14E-03	14.951	0.998	0.213	1.607	0.993	5.24E-02	3.039	0.957
Py_WS_FA(20:1)	Mn	7.53E-03	9.058	0.997	0.353	2.032	0.961	8.15E-02	1.913	0.988
	Co	2.12E-03	32.741	0.997	0.367	1.672	0.982	2.63E-02	6.614	0.981
	Ni	8.33E-03	11.336	0.995	0.366	1.828	0.970	8.33E-02	2.494	0.986
	Zn	3.72E-03	17.714	0.999	0.197	1.495	0.987	5.05E-02	3.434	0.975
Py_WS_FA(10:1)	Mn	5.20E-03	10.752	0.992	0.260	1.817	0.977	6.15E-02	2.189	0.976
	Co	1.95E-03	32.650	0.997	0.316	1.626	0.980	2.50E-02	6.487	0.981
	Ni	1.03E-02	9.151	0.996	0.385	1.951	0.954	9.69E-02	2.055	0.987
	Zn	3.80E-03	13.418	0.996	0.165	1.541	0.977	4.93E-02	2.671	0.979
AC_WS	Mn	2.65E-03	21.686	0.992	0.168	1.436	0.816	4.23E-02	3.865	0.853
	Co	1.34E-03	45.410	0.999	0.215	1.431	0.986	2.06E-02	8.283	0.977
	Ni	4.30E-03	18.646	0.999	0.221	1.471	0.969	5.69E-02	3.613	0.996
	Zn	1.75E-03	34.078	0.993	0.120	1.255	0.977	3.89E-02	4.914	0.986
AC_WS_FA(20:1)	Mn	4.27E-03	16.086	0.995	0.271	1.664	0.966	5.44E-02	3.198	0.957
	Co	1.03E-03	60.155	0.994	0.289	1.484	0.978	1.22E-02	12.033	0.994
	Ni	4.63E-03	16.858	0.993	0.287	1.640	0.990	5.75E-02	3.395	0.983
	Zn	1.12E-03	41.156	0.991	0.097	1.228	0.993	2.16E-02	5.880	0.981
AC_WS_FA(10:1)	Mn	4.24E-03	13.446	0.996	0.222	1.656	0.982	5.34E-02	2.690	0.979
	Co	1.08E-03	54.453	0.991	0.191	1.377	0.992	1.90E-02	9.176	0.946
	Ni	3.78E-03	18.804	0.994	0.210	1.493	0.986	5.04E-02	3.683	0.973
	Zn	1.27E-03	43.458	0.995	0.102	1.210	0.997	3.44E-02	5.517	0.918

References

(1) Mulligan, C. J.; Strezov, L.; Strezov, V. Thermal Decomposition of Wheat Straw and Mallee Residue under Pyrolysis Conditions. In *Energy and Fuels*; 2010; Vol. 24, pp 46–52. https://doi.org/10.1021/ef9004797.

(2) Montero, G.; Coronado, M. A.; Torres, R.; Jaramillo, B. E.; García, C.; Stoytcheva, M.; Vázquez, A. M.; León, J. A.; Lambert, A. A.; Valenzuela, E. Higher Heating Value Determination of Wheat Straw from Baja California, Mexico. *Energy* **2016**, *109*, 612–619. https://doi.org/10.1016/j.energy.2016.05.011.

(3) Ghaly, A. E.; Al-Taweel, A. Physical and Thermochemical Properties of Cereal Straws. *Energy Sources* **1990**, *12* (2), 131–145. https://doi.org/10.1080/00908319008960195.

(4) Cuiping, L.; Chuangzhi, W.; Yanyongjie; Haitao, H. Chemical Elemental Characteristics of Biomass Fuels in China. *Biomass and Bioenergy* **2004**, *27* (2), 119–130. https://doi.org/10.1016/j.biombioe.2004.01.002.

(5) Biswas, B.; Pandey, N.; Bisht, Y.; Singh, R.; Kumar, J.; Bhaskar, T. Pyrolysis of Agricultural Biomass Residues: Comparative Study of Corn Cob, Wheat Straw, Rice Straw and Rice Husk. *Bioresour. Technol.* **2017**, *237*, 57–63. https://doi.org/10.1016/j.biortech.2017.02.046.

(6) Goldfarb, J. L.; Ceylan, S. Second-Generation Sustainability: Application of the Distributed Activation Energy Model to the Pyrolysis of Locally Sourced Biomass-Coal Blends for Use in Co-Firing Scenarios. *Fuel* **2015**, *160*, 297–308. https://doi.org/10.1016/j.fuel.2015.07.071.

(7) Yu, Y.; Xu, M.; Yao, H.; Yu, D.; Qiao, Y.; Sui, J.; Liu, X.; Cao, Q. Char Characteristics and Particulate Matter Formation during Chinese Bituminous Coal Combustion. *Proc. Combust. Inst.* **2007**, *31 II* (2), 1947–1954. https://doi.org/10.1016/j.proci.2006.07.116.

(8) Liu, G.; Vassilev, S. V.; Gao, L.; Zheng, L.; Peng, Z. Mineral and Chemical Composition and Some Trace Element Contents in Coals and Coal Ashes from Huaibei Coal Field, China. *Energy Convers. Manag.* **2005**, *46* (13–14), 2001–2009. https://doi.org/10.1016/j.enconman.2004.11.002.

(9) Koukouzas, N.; Hämäläinen, J.; Papanikolaou, D.; Tourunen, A.; Jäntti, T. Mineralogical and Elemental Composition of Fly Ash from Pilot Scale Fluidised Bed Combustion of Lignite, Bituminous Coal, Wood Chips and Their Blends. *Fuel* **2007**, *86* (14 SPEC. ISS.), 2186–2193. https://doi.org/10.1016/j.fuel.2007.03.036.

(10) Goodarzi, F. Characteristics and Composition of Fly Ash from Canadian Coal-Fired Power Plants. *Fuel* **2006**, *85* (10–11), 1418–1427. https://doi.org/10.1016/j.fuel.2005.11.022.

(11) Kutchko, B. G.; Kim, A. G. Fly Ash Characterization by SEM-EDS. *Fuel* **2006**, *85* (17–18), 2537–2544. https://doi.org/10.1016/j.fuel.2006.05.016.